The dust temperature and density distributions of B68

M. Nielbock, R. Launhardt, J. Steinacker, A. M. Stutz, Z. Balog, H. Beuther, J. Bouwman, Th. Henning, P. Hily-Blant, J. Kainulainen, O. Krause, H. Linz, N. Lippok, S. Ragan, C. Risacher, A. Schmiedeke

The observing programme

As part of the Herschel GTKP "*The earliest phases of star formation*" (EPOS, PI: O. Krause, MPIA), we have observed the prototype of prestellar cores B68 at 100, 160, 250, 350, and 500 µm, using the PACS and SPIRE imagers of the Herschel Space Telescope.

These observations close the gap of the important spectral range, where B68 reaches its emission peak. The Herschel maps cover for the first time the transition between absorption and emission. In particular, the PACS maps show a surprising crescent shaped morphology that deviates from the symmetric configuration already known from extinction and submm data.

Ancillary data were added to derive dust temperature and density maps by employing a ray-tracing algorithm that allows us to model these quantities from the centre to the edge.

The next steps will include a full 3D radiative transfer modelling of B68 and a detailed analysis of the properties of the neighbouring cores that perhaps once belonged to the same filament.

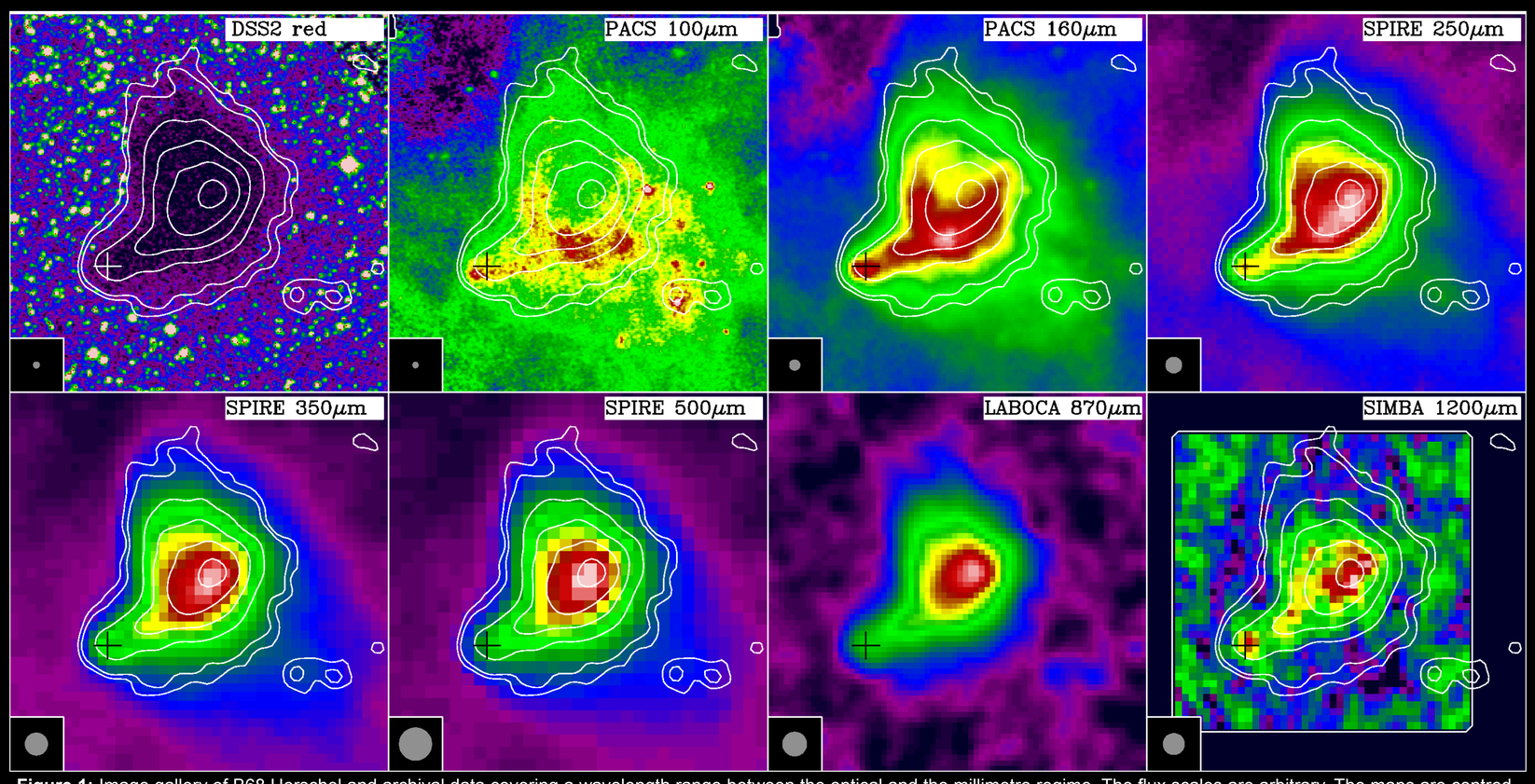

Figure 1: Image gallery of B68 Herschel and archival data covering a wavelength range between the optical and the millimetre regime. The flux scales are arbitrary. The maps are centred on RA=17^{h}22^{m}39^s, Dec=23°50′00″ and have a FOV of 7′×7′. The white contours are taken from the LABOCA map. The crosses indicate the position of the discovered point source that coincides with a local extinction peak and a kinematically detached pointike object in the CO data.

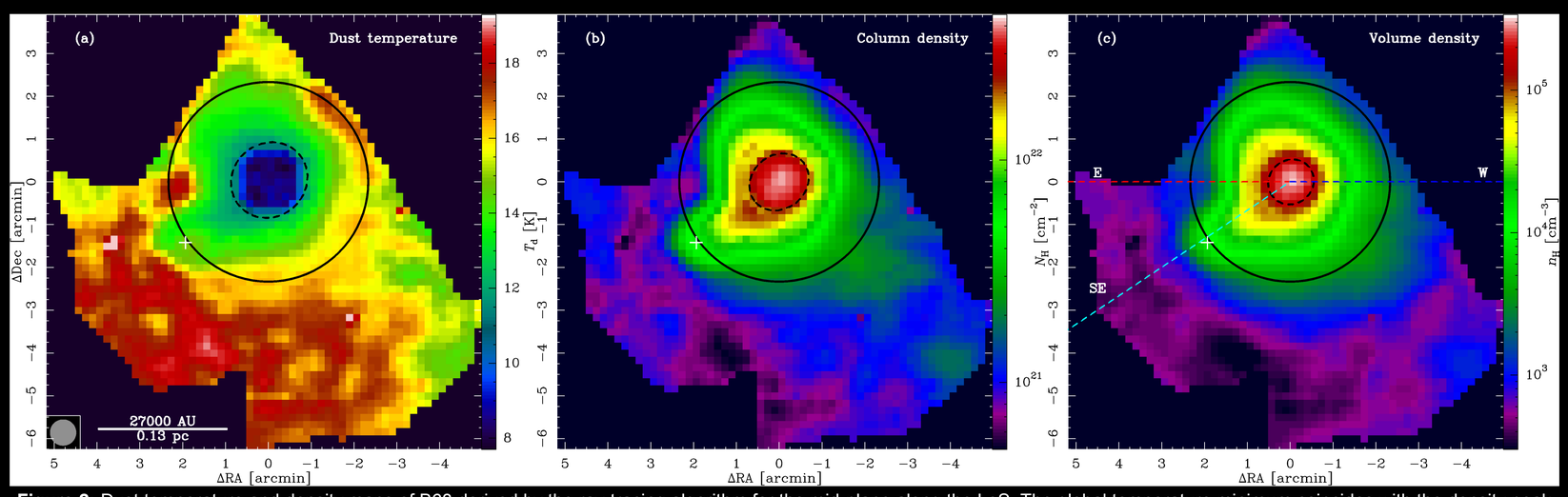

Figure 2: Dust temperature and density maps of B68 derived by the ray-tracing algorithm for the mid-plane along the LoS. The global temperature minimum coincides with the density peak and attains a value of 8 K. The central column density is N_H = 4.6×10^{22} cm^{-2}. The central particle density is n_H = 3.5×10^5 cm^{-3}. The black solid circles represent the size of a Bonnor-Ebert sphere with a radius of 21 000 AU. We have generated three cuts through the maps as dashed lines, whose colours match the ones in the radial profile plots. The white crosses indicate the location of a point source we have identified in the tip of the southeastern trunk by CO observations. The coordinates are given in arcminutes relative to the centre of the density distributions, i.e. RA = 17^{h}22^{m}38. 5^s, Dec = −23°49′50″.

Dust temperature and density distribution

The ray-tracing algorithm yields dust temperatures and densites for every modelling cell. From the resulting data cube, we extract 2D maps of the dust temperature and density distribution for the mid-plane, i.e. the data slice that covers the centre of B68 (Fig. 2).

We find a dust temperature gradient from 8 K in the centre to 17 K at the edge of B68. The central hydrogen column density was found to be N_H=4.6×10^{22} cm^{-2}, and the corresponding volume number density is n_H=3.5×10^5 cm^{-3}.

Summing up the material with $A_V \geq 1$ mag, we find a total mass of 3.2 $M_\odot$ at an assumed distance of 150 pc.

The radial density distribution (Fig. 4) follows a Plummer-like profile (Plummer 1911) with a slope parameter η = 4 as predicted for pressure confined prestellar cores (Whitworth & Ward-Thompson 2001).

$$n_H(r) = \begin{cases} \frac{\Delta n}{\left(1+\left(\frac{r}{r_0}\right)^2\right)^{\eta/2}} + n_{out} & \text{if } r \leq r_{out} \\ 0 & \text{if } r > r_{out} \end{cases}$$

Between the flat density distributions in the centre and the outer tenous halo, we find a density slope that is steeper than $n_H \sim r^{-2}$.

Anisotropic interstellar radiation field

The asymmetric morphology of the emission in the 100 and 160 µm bands can only be explained by surface heating effects caused by a strongly anisotropic interstellar radiation field (ISRF). 3D radiative transfer calculations (Fig. 3) are consistent with an irradiation by the Galactic Centre and the galactic plane.

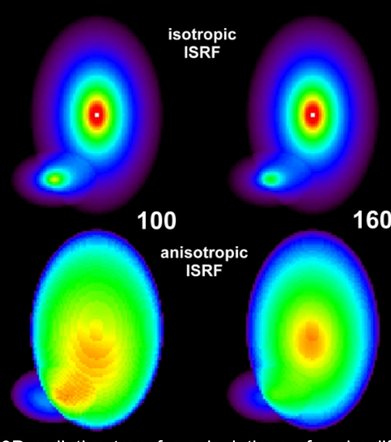

Figure 3: Results of 3D radiative transfer calculations of a simplified model of B68. The asymmetric emission detected in the PACS 100 and 160 µm bands can be explained by surface heating effects produced by an anisotropic ISRF. The main source is the backside illumination by the Galactic Centre. To some extent, the galactic plane that is only 40 pc away and located in the direction of the southeastern extension, also contributes to the anisotropic irradiation.

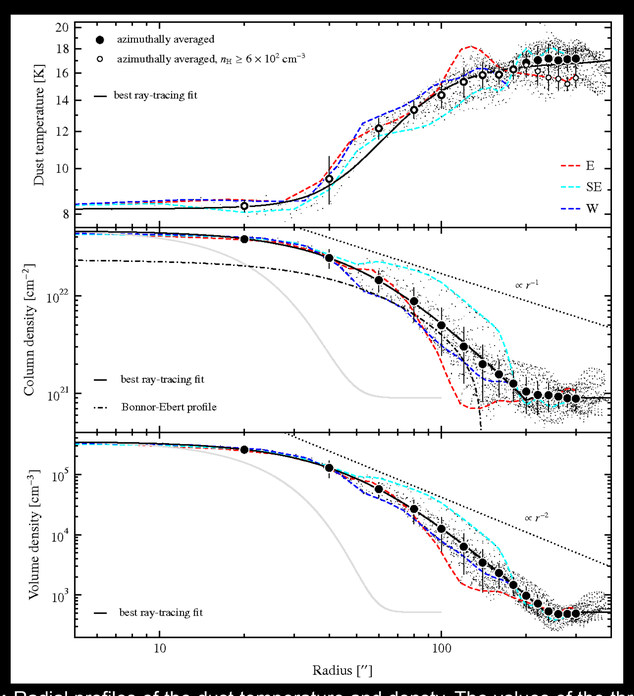

Figure 4: Radial profiles of the dust temperature and densty. The values of the three maps are presented by the small dots. The big filled dots represent azimuthally averaged values. The error bars reflect the 1σ scatter of the azimuthal averaging and hence indicate the deviation from the spheroid assumption. We show the best ray-tracing fits to the data that were used to calculate the three maps, indicated by the solid lines. The coloured dashed lines correspond to the radial cuts along three selected directions, as outlined in Fig. 2 (c). The dotted lines show the canonical density power laws for self-gravitating isothermal spheres, and the grey curve depicts Gaussian profiles that represent the spatial resolution of the maps.

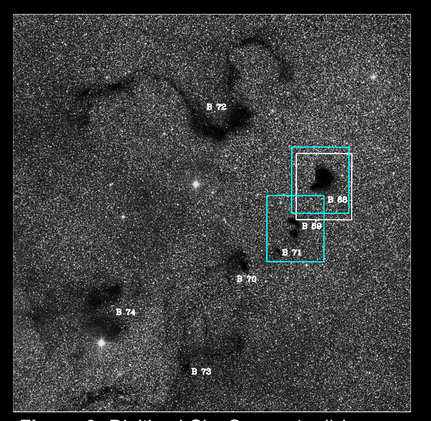

Figure 6: Digitized Sky Survey (red) image of the area around B68 covering a FOV of 1°×1°. The dark clouds B68 to B74 are indicated.

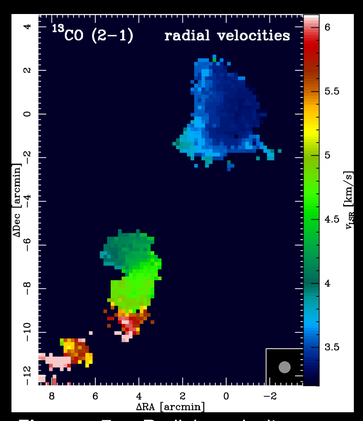

Figure 7: Radial velocity map extracted from ^{13}CO(2-1) observations of B68, B69, and B71 showing a global gradient that is consistent with a flow of common velocities.

Core collision scenario

Burkert & Alves (2009) have developed a scenario of colliding cores in order to explain discrepancies in time scales of stable global oscillations and collapse signatures. According to their picture, the southeastern trunk contains a low mass core – identified as a local maiximum in the extinction map (Alves et al. 2001) – that is colliding with the B68 main body.

In this scenario, B68 is regarded as a former fragment of an already dispersed filament. This view is supported by the radial velocity gradient shown in Fig. 7.

In fact, we have identified at 160 and 250 µm a point source embedded in the tip of the southeastern trunk which appears to be kinematically different from the rest of B68 (Fig. 5). It has the largest redshift within B68 and coincides with the position of the extinction peak. The mass is 8×10^{-2} $M_\odot$.

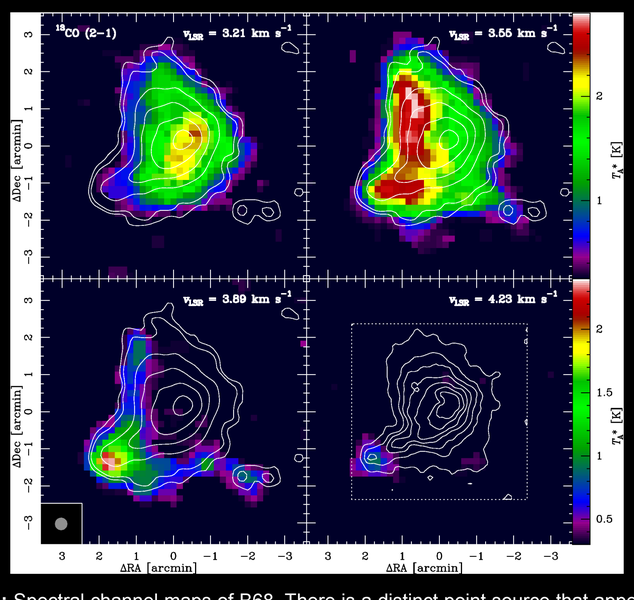

Figure 5: Spectral channel maps of B68. There is a distinct point source that appears at $v_{LSR} \simeq 4$ km s^{-1}. It coincides with a peak in the column density (extinction map, lower right map) at the tip of the southeastern trunk. A rough mass estimate results in 8×10^{-2} $M_\odot$.

The analytic relationship of the radial density profile is nearly identical to the theoretical profile of an isothermal, non-magnetic cylinder (Ostriker 1964). Hacar & Tafalla (2011) have shown that prestellar cores may inherit the proprties of their parental filaments. A similar scenario may be applicable to B68 that appears to be a remnant of a dense fragment of an already dispersed filament. Our CO observations (Fig. 7) show that in addition to oscillations and a low velocity dispersion (e.g. Lada et al. 2003), it appears to belong to a chain of cores showing a common radial velocity gradient.

References

Alves, J. F., Lada, C. J., & Lada, E. A. 2001, Nature, 409, 159
André, P., Ward-Thompson, D., & Motte, F. 1996, A&A, 314, 625
Bergin, E. A., Alves, J., Huard, T., & Lada, C. J. 2002, ApJ, 570, L101
Burkert, A. & Alves, J. 2009, ApJ, 695, 1308
Griffin, M. J. et al., 2010, A&A, 518, L3
Hacar, A. & Tafalla, M. 2011, A&A, 533, A34
Lada, C. J., Bergin, E. A., Alves, J. F., & Huard, T. L. 2003, ApJ, 652, 1366
Ostriker, J. 1964, ApJ, 140, 1056
Plummer, H. C. 1911, MNRAS, 71, 460
Poglitsch, A. et al., 2010, A&A, 518, L2
Whitworth, A. P. & Ward-Thompson, D. 2001, ApJ, 547, 317